Electronic Supplementary Material (ESI) for Soft Matter.

Thermophobic Leidenfrost

Ambre Bouillant, Baptise Lafoux, Christophe Clanet & David Quéré

Physique & Mécanique des Milieux Hétérogènes, UMR 7636 du CNRS, ESPCI, 75005 Paris, France.

and

LadHyX, UMR 7646 du CNRS, École polytechnique, 91128 Palaiseau, France.

Supplementary information

We enclose here supplemental data, figures and movies, following the development of the accompanying paper.

1. Parabolic transverse profile of the substrate

Here we characterize the geometry of the brass plate. The substrate is micromachined layer after layer (each layer is 25 µm-deep) with a milling tip of 150 µm in diameter. The geometry is made concave, that is, flat along the x direction and parabolic across its section (y direction). The roughness is decreased using a rubber gum, and the substrate is further cleaned with isopropanol. To check the geometry and smoothness of the substrate, the plate is then scanned with an optical profilometer (ZYGO - bipolar mode) equipped with a 10x interferometric objective. The roughness is only visible at the micrometric scale.

Most importantly, as shown in figure S1, the substrate has a parabolic profile along the y-direction that is described by the curve $z(y) = ky^2$. The curvature C is thus roughly constant in the y-direction, with a value $C \approx 2k \approx 3$ m^{-1}. A levitating drop or disk of dry ice can slightly oscillate in the gutter with a period $T = 2\pi/(Cg)^{1/2} \approx 1.2$ s, as it propels along the x-direction.

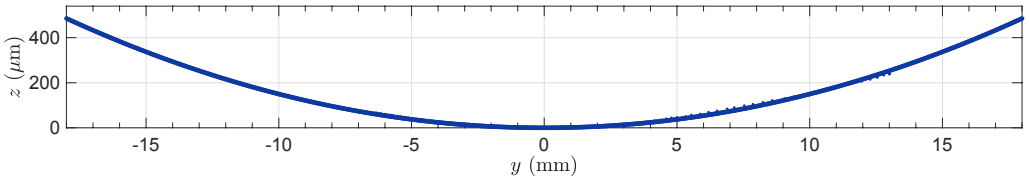

Figure S1. Parabolic profile of the substrate. Transverse profile in the (y,z) plane of the brass bar. The plate is carved by 500 µm, which restricts the trajectories in the x-direction, and it has a parabolic profile $z(y) = ky^2$, with $k = 1.5$ m^{-1}. Hence its curvature is $C = 2k \approx 3$ m^{-1}.

2. Transient and permanent regime of the temperature gradient *G*

Thermal exchanges along the brass bar are dominated by heat diffusion. Laplace equation, integrated between $x = 0$ where $T(0) = T_+$ and $x = L$ where $T(L) = T_-$, leads to a linear variation of the temperature with x. The plate temperature is measured with a side-viewed infrared camera (FLIR A655sc, calibrated on the range [150 ; 450]°C) from the time the side heaters are turned on and onwards. As observed in figure S2, a temperature gradient G establishes along the plate, which, excluding the region too close to the heaters, is roughly constant $|G| \approx 5$°C/cm over the distance L. The duration for the transient regime scales as L^2/D_s, where D_s is the thermal diffusivity of brass ($D_s \sim 10^{-4}$ m^2/s). For $L = 22$ cm, we thus expect typical duration of 10 min for the transient regime, as observed.

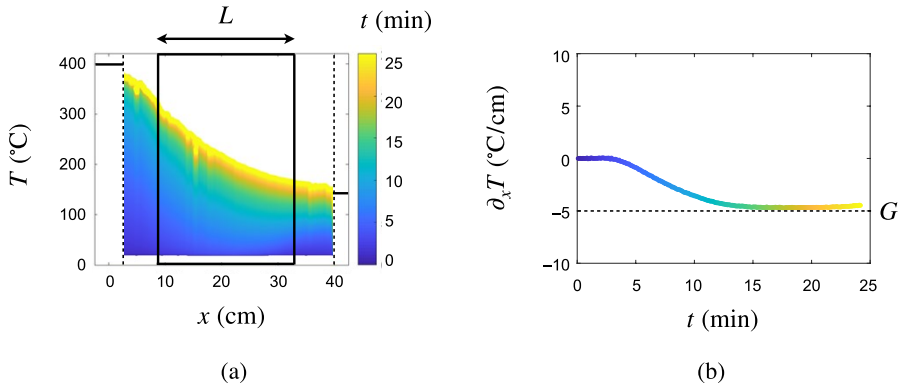

Figure S2: Temperature gradient along the substrate. a. Substrate temperature T along the horizontal x-direction. At $t = 0$, the left heater is set to $T_+ = 400$°C, while the right heater is to $T_- = 150$°C. As time goes on (see the colormap), heat diffuses away from the heaters. After about 10 minutes, a temperature difference of 200°C establishes along the 40 cm-long brass bar. All experiments are performed within the framed region with length $L = 22$ cm, where $T(x)$ is roughly linear. **b.** Temporal evolution of the temperature gradient $G = \partial_x T$, spatially averaged for x ranging from 10 cm to 30 cm. The substrate responds within a delay of 5 minutes to heating; after a transient phase of ~10 minutes, the gradient of temperature becomes roughly constant ($G \sim -5$ °C/cm).

3. Assessment of the slope of the substrate

Here we check that a residual slope along x of the substrate is not responsible for the propulsion of the Leidenfrost drops. To that end, top-view drops trajectories are studied by heating from left to right (temperature gradient $G < 0$) and from right to left ($G < 0$). The acceleration can have multiple origins such as thermophoretic drive or gravity, owing to the unavoidable slope of the substrate or to the thermal expansion of the solid. In figure S3, we report the measured accelerations a (to the cold) of twenty drops with radius $R = 2.6 \pm 0.2$ mm placed on a substrate with $\Delta T = 200$°C, corresponding to the figures 3a and 3b of the accompanying paper.

For $G = -8$ °C/cm, the accelerations (whose distribution can be roughly fitted by a beta function) are peaked around $a = 4.2 \pm 1.4$ mm/s^2. Reverting the sign of the gradient ($G = +8$ °C/cm) sightly shifts the peak in acceleration to $a = 4.6 \pm 0.8$ mm/s^2. If we assume that this difference in a is due to gravitational acceleration $2\alpha_0 g$, we deduce a deviation from horizontality $\alpha_0 \approx 0.05$ mrad, on the order of the precision of our spirit level (< 1 mrad).

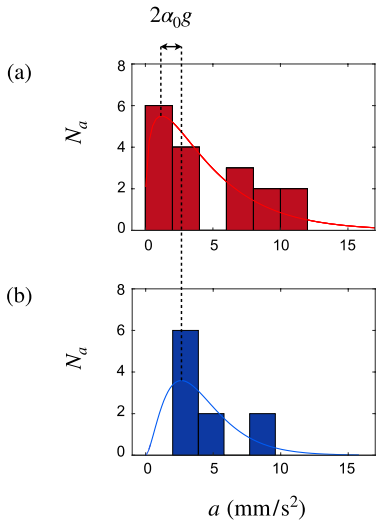

Figure S3. Distributions of acceleration for twenty thermophobic drops with radius $R = 2.6 \pm 0.2$ mm, placed on a substrate subjected to temperature differences of 200°C. Distributions are fitted with beta functions. **a.** For $G = -8$ °C/cm, the accelerations are peaked around $a = 4.2 \pm 1.4$ mm/s^2. **b.** Reverting the gradient sign $G = +8$ °C/cm, the peak in acceleration moves to $a = 4.6 \pm 0.8$ mm/s^2. Attributing the difference between the accelerations to a gravitational acceleration $2\alpha_0 g$, we deduce a plausible deviation from horizontality $\alpha \approx 0.05$ mrad. The corresponding trajectories are displayed in figure 3a and 3b of the accompanying paper.

The differential thermal expansion of the solid can also tilt it. Brass has a (low) linear expansion coefficient $\beta \approx 20$ μK^{-1}. If a rectangular block with volume $\Omega = \zeta l L$ (ζ, l and L being the block thickness, width and length) is homogeneously heated, it isotropically expands and its volume increases by $\delta\Omega \approx 3\beta\Omega\delta T$. When subjected to a horizontal temperature difference ΔT, expansion becomes anisotropic. The hot side rises by $\sim\beta\Delta T$ above the cold side, which generates a tilt $\alpha_\beta \sim \beta\Delta T\zeta /L$. With $\zeta = 1$ cm, $L = 30$ cm, and $\Delta T \approx 200$°C, we predict $\alpha_\beta \sim 0.1$ mrad. As sketched in figure S4, this angle can be accessed by projecting a laser point on the reflective substrate and collecting the light on a screen located at a distance $D = 3$ m where we measure its height z_s. The laser hits the brass plate at $x = L/2$ with an incident angle α_i. When the brass plate is homogeneously heated at a temperature $T = (T_+ + T_-)/2 \approx 275$°C, light is reflected by the same angle α_i. We record the corresponding distance z_s and apply at $t = 0$ the horizontal temperature difference $\Delta T \approx 200$°C (the plate being 25 cm long, the corresponding gradient is 7°C/cm). As shown in figure S4c, the laser point moves down on the screen by δz_s. Despite large fluctuations (displayed in light blue, accounted for the spreading of the laser spot and the mirage effect above the hot plate), its mean value is clearly visible and found to be 0.4 mm after roughly 10 minutes. In the limit of small deviation, $\alpha_\beta << 1$, we simply have $\delta z_s \sim 2\alpha_\beta D$. The deviation induced by inhomogeneous thermal expansion is thus on the order of 0.1 mrad, which generates an acceleration $\alpha_\beta g$ of order 1 mm/s^2, significantly smaller than the accelerations of about 5 mm/s^2 measured in our experiments.

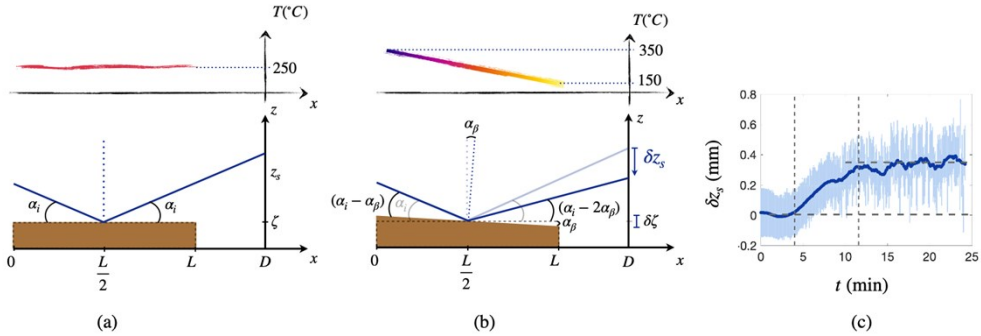

Figure S4. Thermal expansion of the substrate. a. Homogeneous expansion: the substrate temperature is raised by ΔT, which increases its thickness ζ by $\beta\Delta T\zeta$, denoting β as the coefficient of linear thermal expansion. The expansion is measured by reflecting a light beam with incident angle α_i and placing a screen placed at $x = D + L/2$. **b.** Horizontal thermal gradient $G < 0$. The plate expands anisotropically, leading to a net tilt $\alpha_\beta \sim \beta\Delta T\zeta/L$. The laser incidence on the tilted plate is $(\alpha_i - \alpha_\beta)$, and it reflects to an angle $(\alpha_i - \alpha_\beta)$ with respect to the horizontal, causing a downward shift of the light spot on the screen by $\delta z_s \sim 2\alpha_\beta D$. **c.** Temporal evolution of the laser deflection δz_s after the temperature gradient is applied. The material evolves during ~10 minutes and the deflection saturates at an average distance $\delta z_s \approx 0.4$ mm. Fluctuations, in light blue, arise from the beam spreading along with variations of the refractive index of air induced by temperature variations above the plate (mirage effect).

4. Does thermophobia persist in the capillary limit of self-propelled droplet?

In this section, we question whether the thermophoretic thrust can also affect the trajectory of Leidenfrost droplets smaller than the capillary length κ^{-1}. As recently reported, millimetric droplets without external stimuli self-rotate and self-propel in the direction fixed by their rotation, a random quantity on an isothermal flat substrate [5]. A Leidenfrost drop hosts strong internal flows that become asymmetric when the drop is quasi-spherical. In order to check whether this self-propulsion impacts the thermophobic effect, we perform the experiment described in figures 1 and 2 for $R < \kappa^{-1}$ on a substrate with $T_+ = 350$°C and $T_- = 150$°C ($G \approx -8$°C/cm). Figure S5 collects and compares the top-viewed trajectories obtained in the reference case of large drops ($R \gtrsim 2$ mm, a) with that obtained for quasi-spherical droplets ($R \approx 1$ mm, b). In both cases, the liquid leaves it initial position with roughly straight trajectories. Denoting β as the mean direction it follows (averaged over the entire path), the experiment reveals a marked difference in the behavior depending on the drop size. When large drops all head toward the cold, smaller drops propel in all directions. The histogram of these directions displayed in figure S5c quantified this trend. On the one hand, large drops move to the cold (red bin at $\beta = 0$). On the other hand, millimetric droplets keep on self-propelling in random directions (blue bins spread from $|\beta| = 0$ to 180°): not only some of them head toward the hot ($|\beta| = 180$°), but, remarkably, they can even overcome the gutter lateral slope. This experiment reveals that the self-propulsion observed for these quasi-spherical drops persist, the tilt of the base induced by internal rolling being of larger amplitude than the tilt induced by differential erosion. The tilt and acceleration

reported in [5] were on the order of 5 mrad and 50 mm/s^2, respectively, that is 10 times larger than the thermophoretic acceleration at stake here. This is confirmed in figure S5d, where we represent the acceleration histograms obtained on the thermal ramp, comparing the regime of flattened drops on an isothermal, flat plate, for which we do not expect motion, and the capillary regime, for which we expect self-rotation and self-propulsion. Again, large drops are directed toward the cold, while quasi-spherical drops move in all directions. Alike on flat plates, thermophobic drops propel with accelerations smaller than self-propelled droplets. However, we notice that accelerations are further spread than reported in [5] and that quasi-spherical droplets trajectories are slightly biased to the cold. The lateral curvature of the plate and the thermophoretic force may add to the self-propelling force or even bias the rolling direction, ordinarily randomly set when the inner flow symmetry breaks. We conclude that in the hitherto-unexplored limit where Leidenfrost drops are reshaped into spheres by capillarity, the thermophoretic force remain small compared to the self-propelling force.

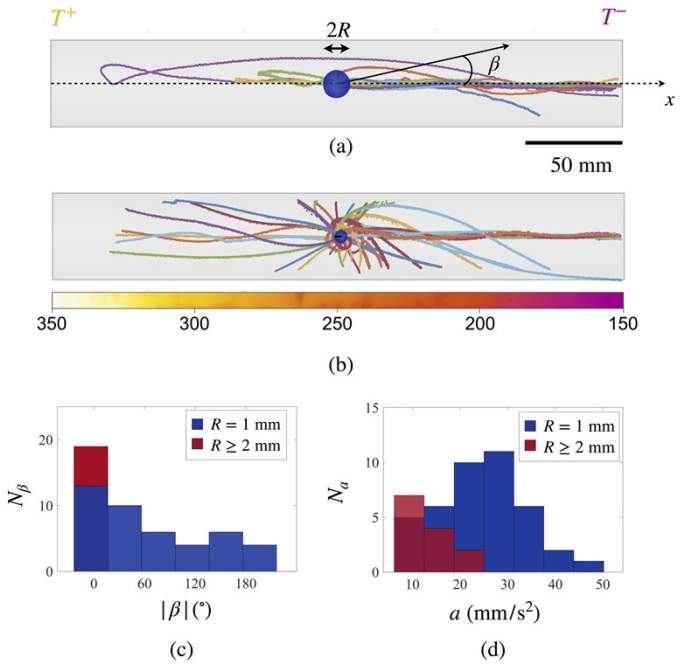

Figure S5: Leidenfrost drops with various sizes on a temperature gradient. a. Experiment viewed from the top: twenty water drops with radius $R \gtrsim 2$ mm (flattened by gravity) are dispensed from a needle ($H \approx 4$ mm) at the centre of the inhomogeneously heated brass plate ($G \approx -8$°C/cm). Their successive paths, distinguished by colours, confirm the thermophobic behaviour. **b.** Same experiment in the regime of quasi-spherical drops ($R \approx 1$ mm). The fifty trajectories show that droplets are not systematically attracted toward the cold. **c.** Histograms of the mean propelling direction |β| (in degree, |β| = 0 points the cold side and |β| = 180°, the hot side) and of the liquid acceleration a (deduced by fitting the trajectories with parabola), for $R \gtrsim 2$ mm (red, data are spread due to the disparity in R) and for $R \approx 1$ mm (blue).

5. Behavior of Leidenfrost solids

Here, we consider the trajectory of Leidenfrost solids (dry ice). Figure S6a reports the successive positions of a centimetric rectangular block with mass m = 3.6 g. Dry ice is first immobilized with a ring after it is placed on a non-uniformly heated substrate. Once the ring is lifted ($t = 0$), ice accelerates toward the cold and we deduce from top views its x and y positions (figure S6b). The function $x(t)$ is parabolic, $x(t) = at^2/2$, with $a = 6.8 \pm 0.1$ mm/s^2, that is, on the same order of magnitude as measured for water. The y position, shown in the insert, highlights the transversal oscillations (period of 1.8 s and amplitude of a few millimeters), again similar to that observed with water.

The instantaneous velocity U can be obtained by deriving the function $x(t)$. Figure S6c shows that U increases linearly with time, confirming that the solid is subjected to a uniform force. The initial velocity is slightly larger than zero, due to the difficulty to start strictly from rest with our trapping technique. These behaviors are reproducible, as shown in figure S6d where we follow fifty solids: all trajectories are parabolic, and heading to the cold. However, the disparities in the block geometry, the existence of an initial velocity and the spinning within the horizontal plane are obstacles to a quantitative analysis of the trajectories.

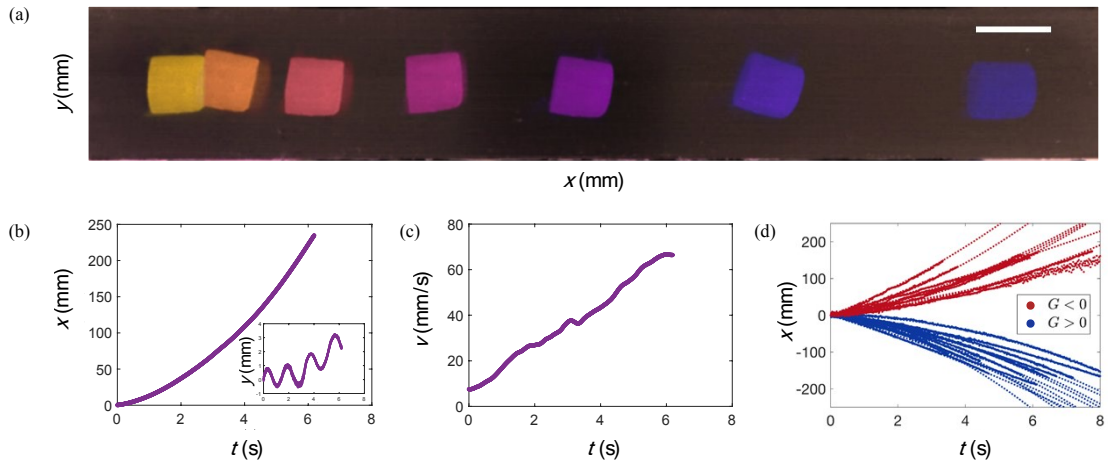

Figure S6. Dry ice on a thermal gradient. a. Top-view chronophotography showing a block of dry ice (m = 3.6 g), starting at a place where we have $T_0 \approx 350$°C and propelling to the cold where we have $T_- \approx 100$°C. The temperature gradient is $G \approx -7$°C/cm. Interval between successive photos is 0.8 s, colors are used to better distinguish them and the bar indicates 5 cm. **b.** Position x as a function of time t for the same experiment; $x(t)$ is quadratic, $x(t) = at^2/2$, and we deduce from the fit $a = 6.8 \pm 0.1$ mm/s^2. The insert shows regular oscillations in the y-direction (period of 1.8 s) related to the parabolic curvature of the substrate. **c.** Instantaneous velocity $U(t)$ derived from $x(t)$; $U(t)$ is (roughly) linear in time. **d.** Superimposition of ~50 trajectories for Leidenfrost disks or rectangular blocks with various dimensions. All ices are uniformly accelerated with $a \sim 2$–10 mm/s^2 along the x direction when $G < 0$ (red) or in the opposite direction when $G > 0$ (blue).

6. Discussion on the subsidiary dependence of vapor properties with T

Temperature variations along the vapor cushion were mainly supposed to only affect the evaporation rate and not the vapor properties. The temperature profile within the thin vapor layer is hard to predict since the vapor flow couples with heat exchange from the substrate to the liquid. Since the evaporating interface is isothermal, vapor undergoes temperature variations on the order of $(T - T_b) \approx 200°C$ (or K) by roughly 50 μm. As commonly assumed, vapor properties are considered constant and taken at the average temperature $(T + T_b)/2 \approx 200°C$ (or 473 K) – as done in table S1 below, for instance.

	H_2O	CO_2
Boiling/sublimating temperature $T_{b,s}$(°C)	100	-80
Vapor density ρ_v (kg/m^3)	0.45	1.98
Condensed phase density ρ (kg/m^3)	958	1560
Vapor thermal conductivity λ (mW/K/m)	32	17
Vapor specific heat C_p (J/kg/K)	2000	850
Latent heat L (J/kg)	$2.2\ 10^6$	$5\ 10^5$
Vapor dynamic viscosity η_v (Pa.s)	$1.6\ 10^{-5}$	$2.2\ 10^{-5}$
Liquid surface tension γ(mN/m)	60	-
Capillary length κ^{-1} (mm)	2.5	-

Table S1: Physical properties of water and carbon dioxide in the vapor and condensed (liquid or solid) phases.

We wonder how vapor properties respond to a horizontal temperature difference G□ and impact the tilt at the drop base. We focus on thermal dependences of the vapor conductivity λ, dynamic viscosity η_v and density ρ_v (or kinematic viscosity $\nu_v = \eta_v/\rho_v$). Vapor is assumed to be an ideal gas for which the heat capacity C_p is independent of T. According to the kinetic theory, the thermal diffusivity $\lambda/\rho_v C_p$ and the kinematic viscosity ν_v scale as the product of the mean free path Λ by the root-mean-square velocity $\langle v \rangle$ of the molecules. $\Lambda \sim 1/nS$ is the average distance a molecule travels between collisions, where $n = \rho_v N_a / M$ is the number of molecules per unit volume (independent of T), S the collision cross section (characteristic of the gas), N_a the Avogadro number and M the molecular mass. Since the velocity $\langle v \rangle$ scales as $(R_g T/M)^{1/2}$, R_g being the ideal gas constant, we expect that both vapor conductivity λ and dynamic viscosity η_v scale as $T^{1/2}$. Finally, the ideal gas equation provides the vapor density $\rho_v = pM/R_g T$.

Since $\varepsilon(T) \sim [\lambda \eta_v \Delta T^2 / \rho_v \rho g h L]^{1/4}$, the variations in λ, η_v and ρ_v induced by a temperature horizontal difference G would reinforce the tilt by an angle $\delta\alpha = ¼ [\delta\lambda/\lambda + \delta\eta_v/\eta_v - \delta\rho_v/\rho_v]\varepsilon/$. This yields $\delta\alpha = \sim ½ [G/T] \varepsilon/$. With $G \approx 5°C$, $\varepsilon \approx 50$ μm and ≈ 5 mm, we obtain $\delta\alpha \approx 0.05$ mrad, on the order of 10% of the tilt directly expected from the existence of a gradient ($\alpha \sim G\varepsilon/\Delta T$). The variations of the vapor properties variations would cumulatively reinforce the effect by only roughly 10%, which justifies our choice to privilege the differential erosion as a main source of propulsion.

Captions of the movies

Movie 1. Airflows above the bar brought to 300°C on the left and to 200°C on the right. Tracers reveal thermal upward flows with velocities on the order of 20 cm/s. The bar indicates 2 cm and the movie is slowed down by a factor 5.

Movie 2. Top view of the experiment shown in Figure 1. A water drop with $R = 2.6$ mm, deposited at $x_0 = 8$ cm on a plate with gradient $G \approx -9°C/cm$, spontaneously accelerates toward the cold, along the gutter main axis. When it reaches the position x_L such that $T(x_L) \approx T_L$, it suddenly boils, fragments and quickly evaporates. The dispensing system is slightly blurred as it is out of field. The bar indicates 2 cm and the movie is played in real time.